Biochemical Pharmacology 79 (2010) 463–470

Contents lists available at ScienceDirect

Biochemical Pharmacology

journal homepage: www.elsevier.com/locate/biochempharm

Werner's syndrome helicase participates in transcription of phenobarbital-inducible *CYP2B* genes in rat and mouse liver

Antoine Amaury Lachaud [a,b,1], Sacha Auclair-Vincent [a,b], Laurent Massip [a,c,2], Étienne Audet-Walsh [a,b,3], Michel Lebel [a,c], Alan Anderson [a,b,*]

[a] Centre de recherche en cancérologie de l'Université Laval, L'Hôtel-Dieu de Québec, CHUQ, Québec, Canada
[b] Département de biologie, Université Laval, Québec, Canada
[c] Département de biologie moléculaire, biochimie médicale et pathologie, Université Laval, Québec, Canada

ARTICLE INFO

Article history:
Received 19 June 2009
Accepted 1 September 2009

Keywords:
Phenobarbital-inducible genes
Werner's syndrome
Chromatin immunoprecipitation
Gene regulation
Transcription
Liver

ABSTRACT

Werner's syndrome (WS) is a rare human autosomal recessive segmental progeroid syndrome clinically characterized by atherosclerosis, cancer, osteoporosis, type 2 diabetes mellitus and ocular cataracts. The *WRN* gene codes for a RecQ helicase which is present in many tissues. Although the exact functions of the WRN protein remain unclear, accumulating evidence suggests that it participates in DNA repair, replication, recombination and telomere maintenance. It has also been proposed that WRN participates in RNA polymerase II-dependent transcription. However no promoter directly targeted by WRN has yet been identified. In this work, we report mammalian genes that are WRN targets. The rat *CYP2B2* gene and its closely related mouse homolog, *Cyp2b10*, are both strongly induced in liver by phenobarbital. We found that there is phenobarbital-dependent recruitment of WRN to the promoter of the *CYP2B2* gene as demonstrated by chromatin immunoprecipitation analysis. Mice homozygous for a *Wrn* mutation deleting part of the helicase domain showed a decrease in basal and phenobarbital-induced CYP2B10 mRNA levels compared to wild type animals. The phenobarbital-induced level of CYP2B10 protein was also reduced in the mutant mice. Electrophoretic mobility shift assays showed that WRN can participate in the formation of a complex with a specific sequence within the *CYP2B2* basal promoter. Hence, there is a WRN binding site in a region of DNA sequence to which WRN is recruited in vivo. Taken together, these results suggest that WRN participates in transcription of *CYP2B* genes in liver and identifies the first physical interaction between a specific promoter sequence and WRN.

1. Introduction

Werner's syndrome (WS) is a rare human autosomal recessive disorder that mimics many but not all features of premature aging. It is referred to as a segmental progeroid syndrome because it impacts on a number of organ systems and tissues [1]. It is characterized clinically by atherosclerosis, predisposition to cancer, osteoporosis, type 2 diabetes mellitus, and ocular cataracts [2,3]. The WS gene (*WRN*) was identified in 1996 by positional cloning [4] and codes for a RecQ helicase (WRN) [5]. The human *WRN* gene and its mouse ortholog *Wrn* are widely if not ubiquitously expressed [4,6]. The WRN protein possesses a 3′–5′ exonuclease activity in addition to its 3′–5′ helicase activity [7,8]. Fifty different mutations of the *WRN* gene have been reported from WS patients and all but two result in a truncated protein with loss of the nuclear helicase and exonuclease activities [9,10]. The two exceptions are missense mutations in the exonuclease domain that result in instability of the protein [10]. Although the exact functions of the WRN protein and the molecular deficiencies involved in the clinical phenotype of WS remain

Abbreviations: Ab, antibody; CAR, constitutive androstane receptor; C/EBPα, CCAAT/enhancer binding protein α; ChIP, chromatin immunoprecipitation; EMSA, electrophoresis mobility shift assay; FXR, farnesoid X receptor; GAPDH, glyceraldehyde-3-phosphate dehydrogenase; HPRT, hypoxanthine phosphoribosyl transferase; LXR, liver X receptor; PXR, pregnane X receptor; NF1, nuclear factor 1; oligo, oligonucleotide; PB, phenobarbital; PBRU, phenobarbital response unit; PBREM, phenobarbital responsive enhancer module; PEPCK, phosphoenolpyruvate carboxykinase; Pol II, RNA polymerase II; RXR, retinoid X receptor; TBS, Tris buffered saline; WS, Werner's syndrome; WRN, WS protein.

* Corresponding author at: Centre de recherche en cancérologie de l'Université Laval, L'Hôtel-Dieu de Québec, 11 côte du Palais, Québec, G1R 2J6, Canada. Tel.: +1 418 6915281; fax: +1 418 6915439.
E-mail address: Alan.Anderson@bio.ulaval.ca (A. Anderson).
[1] Present address: Biopredic International, 8-18 rue Jean Pecker, 35000 Rennes, France.
[2] Present address: LBCMCP, CNRS UMR 5088, Université Paul Sabatier, 31062 Toulouse Cedex, France.
[3] Present address: Centre de recherche en endocrinologie moléculaire et oncologique, CHUL, CHUQ, 2705 boulevard Laurier, Québec, G1V 4G2, Canada.

0006-2952/$ – see front matter © 2009 Elsevier Inc. All rights reserved.
doi:10.1016/j.bcp.2009.09.002

unclear, accumulating evidence suggests that it participates in DNA repair, replication, recombination, and telomere maintenance [11,12]. In addition, experiments by Bohr's group using WS lymphoblastoid cell lines carrying homozygous *WRN* mutations showed that global transcription efficiency was reduced to 40–60% of that in cells from normal individuals [13]. Other experiments from the same group using cDNA microarrays showed that the transcription defect in WS primary fibroblast cell lines was specific to certain genes and that the transcriptional changes in such cell lines were strikingly similar to those in cells from aging donors [14]. Similar conclusions were reached from a more extensive recent study using small interfering RNA to reduce WRN synthesis in normal human fibroblasts [15,16]. The contribution of the transcriptional deficit in WS cells to the clinical phenotype is presently not known. Nor is it known if WRN is a functionally active component of the RNA polymerase II (Pol II) machinery or whether its absence or depletion modifies overall cell physiology resulting in diminished transcription efficiency. This latter possibility seems to be ruled out however, because the expression of a minority of genes is increased in cells in which WRN is absent or depleted [14,15].

The barbiturate phenobarbital (PB) is a widely used antiepileptic drug, although it has now been largely superseded in industrialized countries by other agents because of concern about adverse effects [17]. In the liver, PB induces a large spectrum of drug metabolizing enzymes, most notably cytochrome P450 proteins of the 2B subfamily (CYP2B proteins) in mice and rats [18,19]. In PB-treated rats, the hepatic levels of the closely related CYP2B1 and CYP2B2 proteins are increased by 200-fold and 27-fold respectively compared to untreated animals [20,21]. The DNA sequences of the regulatory and coding sequences of rat *CYP2B1* and *CYP2B2* genes are ~97% identical such that they are sometimes referred to as *CYP2B1*/*CYP2B2* in conditions where their sequences cannot be distinguished. In mouse liver, the increase after PB treatment of the CYP2B10 protein, a closely related homolog of the rat CYP2B1 and CYP2B2 forms [22], is about 50-fold [23]. Most of the PB-induced increase in rat liver CYP2B proteins is due to increased transcription [24].

Although no cellular protein that is directly targeted by PB has yet been identified [25], the regulatory sequences responsible for the induced expression of rodent *CYP2B* genes have largely been characterized [22,26]. In rat liver, PB inducibility of the *CYP2B1* and *CYP2B2* genes is conferred by the 163-bp PB response unit (PBRU), a multicomponent enhancer localized approximately 2.2 kb upstream of the transcription start sites [27–29]. A 177-bp fragment with properties similar to those of the rat PBRU is present in the homologous region of the mouse *Cyp2b10* gene [30], and contains a 162-bp segment that is 92% identical to the *CYP2B2* PBRU [31]. A 51-bp PB responsive enhancer module (PBREM) [32] within the PBRU confers PB responsiveness comparable to that of the full-length PBRU in primary hepatocytes when placed directly adjacent to a heterologous promoter [31,32].

The PBRU contains binding sites for a number of transcription factors [33], most notably 3 DR-4 elements, NR1, NR2 and NR3, recognized by heterodimers of the constitutive androstane receptor (CAR) and the retinoid X receptor (RXR) [34–36] and required for the induction by PB-like inducers [31,34]. The PBREM consists of the NR1 and NR2 sites surrounding a nuclear factor 1 (NF1) site [32]. CAR is normally cytoplasmic in hepatocytes. Following treatment with PB-like inducers it migrates to the nucleus where it is thought to activate transcription of *CYP2B* genes [37]. $Car^{-/-}$ mice have undetectable levels of hepatic CYP2B10 mRNA with or without treatment with PB or PB-like inducers [38].

We report here that in mouse and rat liver WRN participates in the basal and PB-induced transcription of *CYP2B* genes. Taken together, our results suggest that in rodents WRN participates in transcription of hepatic genes in vivo and identifies the first physical interaction between a specific promoter sequence and WRN.

2. Materials and methods

2.1. Animal care and treatment

All animals used in these experiments were males aged 5–8 weeks. The $Wrn^{\Delta hel/\Delta hel}$ mice have been described [39]. Sprague–Dawley rats and C57BL/6 mice were from Charles River Laboratory (St-Constant, Canada). Animals were treated in accordance with the requirements of the Comité de protection des animaux du Centre hospitalier universitaire de Québec (Québec, Canada).

2.2. Plasmids

The WRN expression vector contains the full-length murine WRN cDNA cloned into the pCDNA3.1 vector (Invitrogen, Burlington, Canada). Expression vectors for mouse CAR (pCMX-mCARβ), rat FXR (pCMX-rFXR) and mouse PXR (pCDG-PXR) were from R.G. Evans; those for rat C/EBPα (pCI-rC/EBP) and porcine NF1 (pSK-pNF1) were from L. Belanger; and that for rat LXR (pCMX-rLXRβ) was from J.-A. Gustafsson.

2.3. RNA isolation and analysis

Wild type and $Wrn^{\Delta hel/\Delta hel}$ C57BL/6 mice were treated with PB (100 mg/kg i.p.) or saline and sacrificed 16 h later. Livers were rinsed in PBS, pH 7.2 (Invitrogen, Burlington, Canada), frozen in liquid nitrogen and stored at −80 °C until use. Total RNA isolation was performed using TRIzol reagent (Invitrogen) following the supplier's instructions. For Northern blot experiments, 15 μg of RNA was diluted in RNA loading buffer (Fermentas, Burlington, Canada), denatured by incubating for 10 min at 75 °C and subjected to electrophoresis in 1% agarose–18% formaldehyde gels, then transferred by capillarity to a Genescreen nylon membrane (PerkinElmer, Woodbridge, Canada). RNA was crosslinked to the membranes with ultraviolet light. Membranes were then incubated for 30 min at 65 °C with 20 μg/ml of denatured herring sperm DNA (Invitrogen) in phosphate buffer (0.25 M Na phosphate pH 7.2, 7% SDS, 1 mM EDTA). Mouse CYP2B10 and CYP3A11 mRNAs were detected with a 470-bp HindIII–NcoI fragment of rat CYP2B1 cDNA [40] and a 900-bp fragment of rat CYP3A23 cDNA [41] respectively. Membranes were also hybridized with a GAPDH probe to control for loading. Probes were randomly labeled with ^{32}P-dCTP (PerkinElmer) using a commercial kit (GE Healthcare, Piscataway, NJ, USA). Hybridizations were carried out overnight at 65 °C for 16 h in phosphate buffer. The membranes were then washed three times for 10 min at 65 °C in 20 mM Na phosphate pH 7.2; 5% SDS, 1 mM EDTA, and once for 15 min in 20 mM Na phosphate pH 7.2; 1% SDS, 1 mM EDTA. Hybridization was detected using a Storm 860 Phosphorimager and ImageQuant software (Molecular Dynamics/GE Healthcare, Piscataway, NJ, USA).

For mRNA quantitation using the branched DNA assay, oligonucleotide probes for CYP2B10 were those defined by Cherrington et al. [42]. These probes, as well as those for hypoxanthine phosphoribosyl transferase (HPRT) and all reagents for analysis, were supplied in the QuantiGene 2.0 Reagent System kit (Panomics, Fremont, CA, USA). Total RNA was extracted from frozen liver using the TRIzol reagent. Ten micrograms and 250 ng of total RNA from untreated and PB-treated mice respectively were used for the analyses, which were performed according to the manufacturer's protocol. Luminescence was measured with a Luminoskan Ascent (Thermo Fisher Scientific, Waltham, MA, USA). Quantitative real-time PCR analyses were performed by the

Plateforme de quantification génomique, Centre de recherche du CHUL (Québec, Canada).

2.4. Microsomes and detection of CYP2B proteins by Western blotting

Wild type and $Wrn^{\Delta hel/\Delta hel}$ C57BL/6 mice were treated with PB (100 mg/kg i.p.) or saline and sacrificed 16 h later. Livers were rinsed in cold PBS, frozen in liquid nitrogen and stored at −80 °C until use. Microsomes were isolated [43] and Western blot analysis was performed. Samples of 10 μg of protein per lane were subjected to SDS-polyacrylamide gel electrophoresis on 10% polyacrylamide gels and transferred to PVDF membranes (GE Healthcare) according to the supplier's instructions. After a 1 h incubation in 5% fat-free dried milk in TBS–Tween (20 mM Tris–HCl pH 7.6, 137 mM NaCl, 0.1% Tween 20), CYP2B proteins were detected using a anti-CYP2B1 Ab [44], a gift of David Waxman, that also recognizes mouse CYP2B proteins [45]. Following incubation with horseradish peroxidase-conjugated secondary Ab (GE Healthcare), proteins were detected with ECL Chemiluminescent reagents (GE Healthcare) with X-ray films. For the detection of actin, used as a loading control, the membranes were incubated with the H-196 Ab (sc-7210) from Santa Cruz Biotechnology (Santa Cruz, CA, USA). Actin was detected as an 80-kDa covalent complex with 17β-estradiol dehydrogenase [46]. This complex is present in liver [47] and can be isolated with microsomes [48].

2.5. Chromatin immunoprecipitation (ChIP) analysis

Rat liver chromatin was prepared by formaldehyde perfusion following the protocol of Chaya and Zaret [49] with minor modifications. Briefly, rats were treated with PB (75 mg/kg i.p.) or saline and 16 h later were anesthetized with diethyl ether. Liver perfusion was performed [50] using a peristaltic pump (30 ml/min) with solutions at 37 °C first of PBS, pH 7.2, containing 50 ng/ml heparin (Sigma–Aldrich, Oakville, Canada) for 5 min and then of PBS containing 1% formaldehyde. The formaldehyde was allowed to incubate in the perfused liver for 5 min in the animal. The liver was dissected out, placed in a beaker in an incubator at 30 °C for another 5 min and then minced in 6 ml of glycine-containing buffer A [49] at 4 °C. Nuclei were then purified and sonicated, and chromatin was purified on a CsCl step gradient and dialyzed against 10 mM Tris–HCl (pH 7.5)/10 mM EDTA [49]. Partially sonicated crosslinked chromatin (500 ng/μl final concentration) was digested for 3 h with 500 U of AluI (Fermentas) at 37 °C in a final volume of 2 ml. To ascertain that digestion was complete, an aliquot of digested chromatin was removed, crosslinks were reversed by incubation for 4 h at 65 °C and the DNA was purified by phenol–chloroform extraction and analyzed on a 1% agarose gel. A second type of digestion control was also performed consisting of a PCR analysis using digested and undigested chromatin as template and primers that encompass AluI sites. For immunoprecipitation, performed using a commercial ChIP kit (Uptstate/Millipore, Billerica, MA, USA), 100 μl of digested crosslinked chromatin was diluted in the ChIP dilution buffer (1 ml final volume), precleared by incubation for 1 h at 4 °C after addition of 40 μl of a slurry of salmon sperm DNA–protein A–agarose beads supplied with the kit. After removal of the beads by centrifugation (30 s, 600 × *g*), the preparation was incubated overnight at 4 °C with no Ab or with anti-mWRN AB16489 Ab (Abcam, Cambridge, MA, USA) (in some experiments anti-WRN H-300 primary Ab sc5629 from Santa Cruz Biotechnology was employed and gave similar results) or with anti-Pol II Ab MMS-126R-500 (Cedarlane, Hornby, Canada). After addition of salmon sperm DNA–protein A–agarose beads (40 μl) and incubation for 1 h at 4 °C, beads were recovered by centrifugation. Washes and chromatin elution were performed according to the supplier's instructions. Crosslinks were reversed by incubation overnight at 65 °C and proteins were digested with proteinase K (Fermentas) according to the kit supplier's instructions. DNA was recovered by phenol–chloroform extraction with 20 μg of glycogen (Sigma–Aldrich) as carrier. Immunoprecipitated fragments were analyzed by PCR (incubation at 95 °C for 3 min then 22–25 cycles of 95 °C for 30 s, 55 °C for 30 s, and 72 °C for 30 s) and analyzed on a 1% agarose gel. PCR primers used are given in Supplementary Table 1. Input control samples were obtained by reversing the crosslinks of the same amount of AluI-digested chromatin that was used for the immunoprecipitation.

2.6. Co-immunoprecipitation

WRN, CAR, NF1 and C/EBPα were synthesized in vitro using a TnT-T7 kit (Promega, Montréal, Canada) and were labeled with ^{35}S methionine (PerkinElmer) according to the supplier's instructions. Each assay mixture for co-immunoprecipitation contained 15 μl of in vitro-synthesized WRN from a TnT-T7 reaction mixture and 15 μl of one of the other proteins. The proteins were incubated in 150 μl of buffer Z (25 mM Hepes pH 7.6, 60 mM KCl, 5 mM $MgCl_2$ 10% glycerol, 0.25 mM EDTA pH 8.0, 50 ng/μl bovine serum albumin and 0.5 mM DTT) for 1 h at 4 °C with 20 μl of a slurry of salmon sperm DNA–protein A–agarose beads and then, after the removal of the beads by centrifugation, overnight at 4 °C with 7 μl of anti-WRN Ab solution. For immunoprecipitation, 10 μl of beads was added and incubation was continued for 1 h at 4 °C. The beads were recovered by centrifugation as before and washed seven times with 200 μl of buffer Z. Proteins were eluted by adding 20 μl of Laemli buffer to the beads, and subjected to electrophoresis on an SDS-10% polyacrylamide gel. Images were analyzed using a Storm 860 Phosphorimager and ImageQuant software (Molecular Dynamics/GE Healthcare).

2.7. Electrophoretic mobility shift assay (EMSA)

Proteins were synthesized in vitro using a TnT-T7 kit (Promega). Binding reaction mixtures for analysis contained, in a final volume of 24 μl, 3 μl of TnT-T7 reaction mixture for each protein, ∼150,000 cpm labeled fragment, 12 mM Hepes pH 8.0, 60 mM KCl, 5 mM $MgCl_2$, 0.12 mM EDTA, 12% glycerol, and 5 μg/ml poly-dIdC. Incubations were conducted with or without various amounts of indicated competitor DNAs. Reaction mixtures were incubated on ice for 30 min and subjected to electrophoresis (13 V/cm, 90 min) in 1× Tris borate buffer (82 mM Tris borate/1 mM EDTA, pH 8.0) on 5% acrylamide gels made up in 0.3× Tris borate buffer. Retarded complexes were detected using a Phosphorimager and ImageQuant software.

3. Results

3.1. PB induction of CYP2B10 and CYP3A11 mRNAs and of CYP2B10 protein is reduced in mice that carry a homozygous deletion in the WRN helicase domain

We investigated hepatic CYP2B10 and CYP3A11 mRNA and CYP2B10 protein levels after PB treatment in $Wrn^{\Delta hel/\Delta hel}$ mice carrying a homozygous deletion in the WRN helicase domain [39]. These mice synthesize a WRN protein lacking part of its helicase domain and display several of the abnormal metabolic traits associated with WS [51]. On Northern blots, $Wrn^{\Delta hel/\Delta hel}$ mice displayed a reduction in the PB-induced level of hepatic CYP2B10 mRNA (Fig. 1A). A similar result was observed for the PB-induced mRNA level of another PB-inducible CYP, CYP3A11 [52] (Fig. 1A). In a parallel experiment, basal and PB-induced hepatic CYP2B10 mRNA levels in $Wrn^{\Delta hel/\Delta hel}$ mice, normalized with respect to HPRT mRNA, were quantified by the branched DNA assay [42,53] and

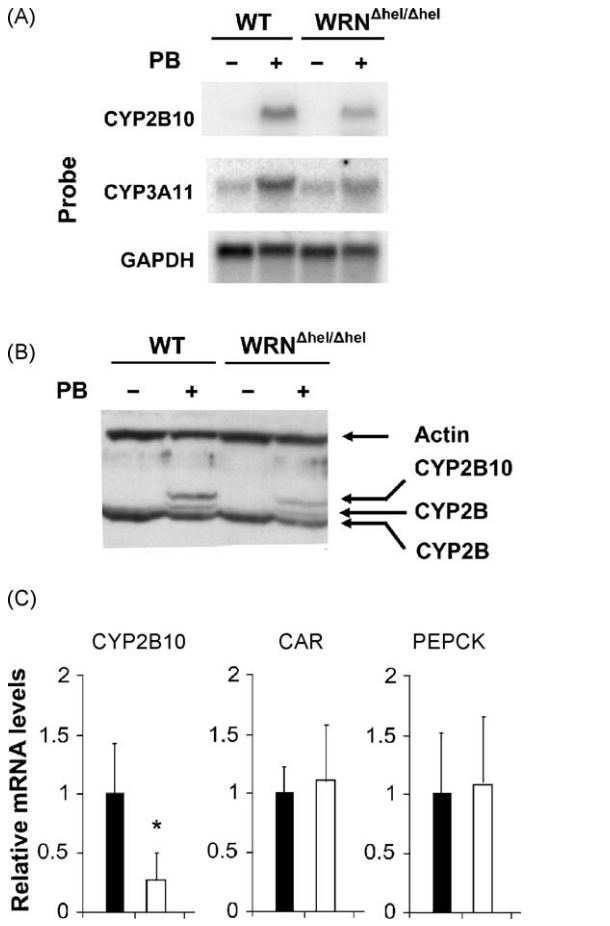

Fig. 1. (A) Northern blot analysis of wild type and $Wrn^{\Delta hel/\Delta hel}$ mouse liver CYP2B10 and CYP3A11 mRNA levels. Wild type and $Wrn^{\Delta hel/\Delta hel}$ mice were treated or not with PB for 16 h and total liver RNA was isolated and subjected to Northern blot analysis. (B) Western blot analysis of wild type and $Wrn^{\Delta hel/\Delta hel}$ mouse hepatic CYP2B10 protein. Wild type and $Wrn^{\Delta hel/\Delta hel}$ mice were treated or not with PB and sacrificed 16 h later. Western blot analysis was performed on liver microsomal proteins. (C) Quantitative real time PCR analysis of levels of hepatic mRNA for CYP2B10, CAR and PEPCK in wild type (WT) (filled bars) and $Wrn^{\Delta hel/\Delta hel}$ (empty bars) mice. mRNA levels were normalized with respect to 18S ribosomal RNA. The levels for wild type animals were set at 1. Results shown are average values (±S.D.) of triplicate assays for three mice in each group. The single asterisk (*) denotes a significant difference ($P < 0.01$) between the CYP2B10 mRNA level in $Wrn^{\Delta hel/\Delta hel}$ mice compared to wild type. Differences were assessed for statistical significance using Student's two-tailed *t*-test, assuming unequal variance.

found to be, respectively, 29% and 67% of those in wild type mice. In an additional parallel experiment with untreated mice, hepatic levels of CAR, phosphoenolpyruvate carboxykinase (PEPCK) and CYP2B10 mRNAs were estimated by quantitative real time PCR. Once again, the CYP2B10 mRNA level in $Wrn^{\Delta hel/\Delta hel}$ mice was reduced to near 30% of the wild type levels, whereas CAR and PEPCK mRNA levels were unchanged (Fig. 1C). The levels of hepatic CYP2B proteins in PB-treated wild type and $Wrn^{\Delta hel/\Delta hel}$ mice were assessed by Western blot analysis. The PB-inducible CYP2B10 protein and an unidentified PB-induced CYP2B protein were notably reduced in the $Wrn^{\Delta hel/\Delta hel}$ mice (Fig. 1B).

3.2. The rat WRN protein is recruited to the CYP2B2 promoter in response to PB administration

To assess whether the WRN protein is recruited to the *CYP2B* locus in hepatic cells after PB treatment, ChIP experiments were performed with liver chromatin from rats treated with saline or PB. The crosslinked liver chromatin was fragmented by partial sonication followed by complete digestion with the restriction enzyme AluI (Fig. 2A and B). The ~2.3-kb *CYP2B2* 5′ flanking and promoter region has 11 AluI sites and they are conserved in *CYP2B1*, which has an additional site in the promoter-proximal fragment (fragment 1 in Fig. 2A). Thus, the promoter-proximal fragment cannot be amplified from AluI-digested *CYP2B1* DNA. To confirm that the AluI digestion of the crosslinked chromatin was complete, PCR analysis was performed with primers that flank AluI restriction sites (Fig. 2C). In the ChIP experiments, a positive signal was obtained using chromatin from PB-treated rats with primers targeting the *CYP2B2* promoter region whereas in chromatin from untreated animals the signal was close to the background (Fig. 2D). Input controls showed that the same amount of hepatic chromatin from treated or untreated rats was used. Primers targeting sequences other than the promoter, either in the *CYP2B1*/*CYP2B2* 5′ flank (Fig. 2D) or in the *CYP2B2* coding sequence (data not shown), did not give positive signals. ChIP analyses using anti-Pol II Ab showed that there was a substantial presence of Pol II in association with the *CYP2B2* promoter in the absence of PB treatment and that Pol II was recruited to same region in response to PB treatment. Taken together, these results indicate that WRN is recruited to the *CYP2B2* promoter in response to PB treatment in rat liver chromatin.

3.3. CAR, FXR, PXR and NF1 can be co-immunoprecipitated with WRN in vitro

The anti-WRN Ab efficiently immunoprecipitated WRN synthesized in vitro, whereas in the absence of added Ab or in the presence of an anti-actin Ab no immunoprecipitate was observed (Fig. 3A). Note that several faster migrating components were present in the in vitro-synthesized WRN preparations (Fig. 3). Similar bands have been seen with in vivo-synthesized WRN [54]. These bands may represent degraded forms of the protein.

WRN has been shown to interact physically or functionally with several proteins involved in different cellular functions, but not with proteins involved in transcriptional processes [55] except for p53 [56]. We assessed the possibility that WRN could bind in vitro to transcription factors that are known or suspected to participate in *CYP2B* transcription, or that are related to them. The factors tested were NF1 and C/EBPα, as well as the nuclear receptors CAR, the farnesoid X receptor (FXR), and the pregnane X receptor (PXR). The *CYP2B1* and *CYP2B2* proximal promoters contain a functional C/EBP binding site [57,58]. No CAR binding site has been reported in the *CYP2B* proximal promoter regions but this transcription factor plays a central role in PB-induced *CYP2B* transcription, and binds to the PBRU, as does NF1 [27]. As seen in Fig. 3B, CAR and NF1, but not C/EBPα, were co-immunoprecipitated by anti-WRN Ab. The association of CAR with WRN raised the possibility that other nuclear receptors might form complexes with WRN. Indeed, FXR and PXR, but not LXR, were co-immunoprecipitated with WRN by the anti-WRN Ab (Fig. 3B). No such immunoprecipitate was detected when the various transcription factors were incubated with the anti-WRN antibody in the absence of WRN (data not shown).

3.4. WRN can form a complex in vitro on the CYP2B2 promoter

As the ChIP results showed that WRN is recruited to the *CYP2B2* proximal promoter in response to PB treatment, we performed EMSA analysis to investigate the possibility that WRN could form a complex in vitro with a 146-bp DNA fragment corresponding to the proximal promoter sequence (Fig. 4A). At least three somewhat diffuse and ill-defined retarded complexes were formed with WRN alone (Fig. 4B, lane 1) or with WRN in combination with CAR (Fig. 4B, lane 2) or with NF1 (Fig. 4B, lane 3). However, when WRN

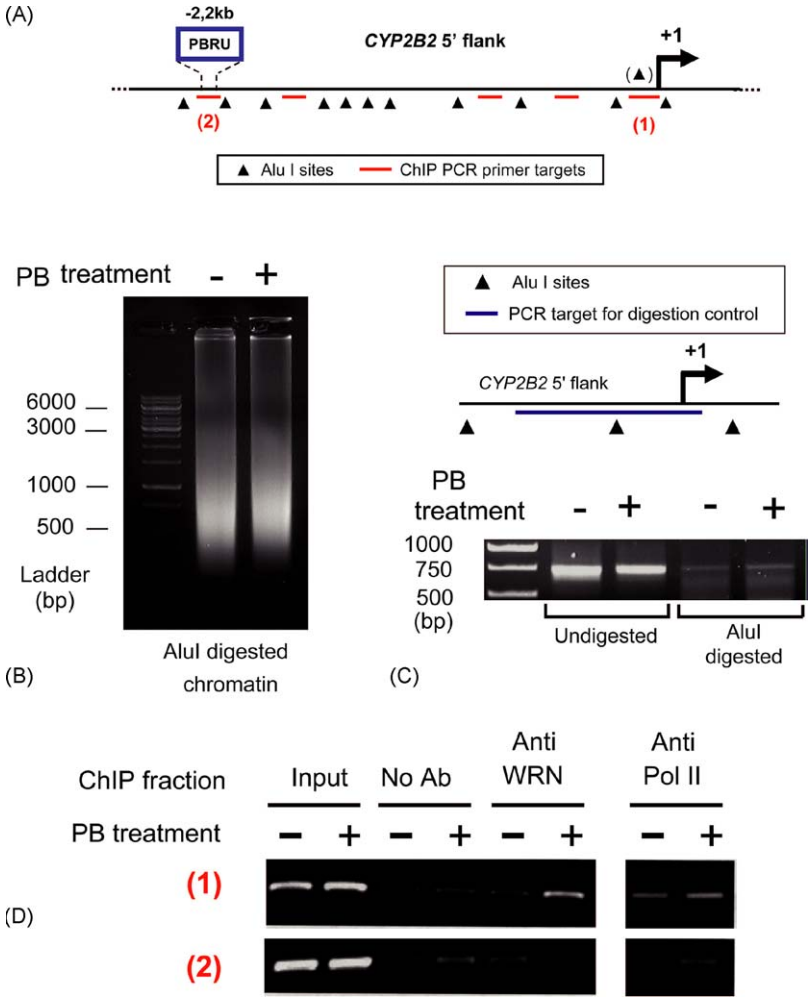

Fig. 2. Rat WRN is recruited to the *CYP2B1*/*CYP2B2* promoters in response to PB treatment. (A) Schematic representation of the *CYP2B2* 5′ flank showing the AluI sites (arrowheads) used for chromatin digestion and the positions of PCR primer targets (see Supplementary Table 1 for primer sequences). The PCR primer targets are conserved in the *CYP2B1* 5′ flank, as are the AluI sites. The *CYP2B1* sequence has an additional AluI site in *CYP2B2* fragment 1 (filled triangle in parenthesis), such that fragment 1 cannot be amplified from *CYP2B1*. Primer sequences are provided in Supplementary Table 1. (B) Control for AluI digestion of crosslinked chromatin. The average length of chromatin fragments is seen to be near 500 bp. (C) Control for AluI digestion efficiency. DNA was recovered from undigested and digested chromatin and used as template for PCR amplification using primers flanking an AluI site as shown. The greatly reduced signal when digested chromatin was used is a measure of the efficiency of the digestion. (D) ChIP PCR analysis. The numbers in parentheses on the left refer to the targets of PCR amplification shown in panel A.

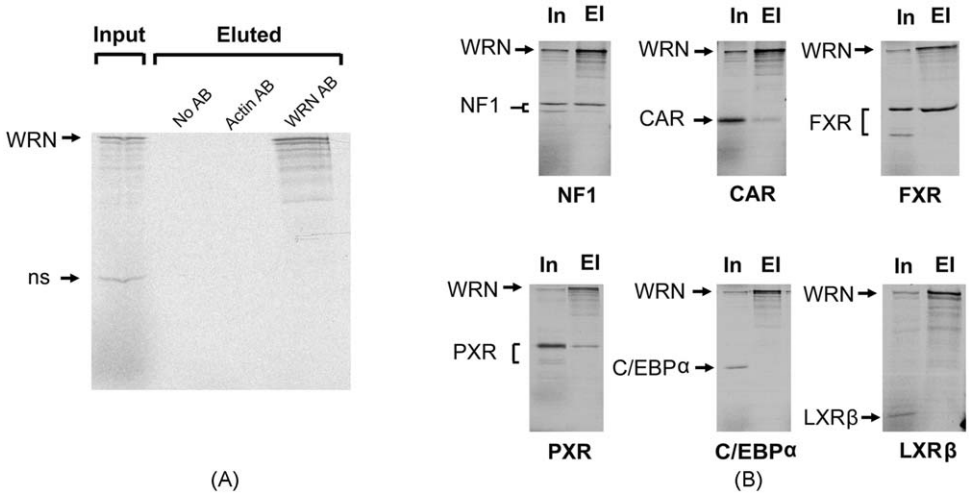

Fig. 3. WRN can bind transcription factors in vitro. Proteins were synthesized in vitro in the presence of ^{35}S methionine. The anti-WRN Ab (Ab 16489, Abcam) was used to immunoprecipitate WRN alone (A) or WRN in the presence of other in vitro-synthesized proteins as shown (B). In, input; El, eluted; ns, non-specific product.

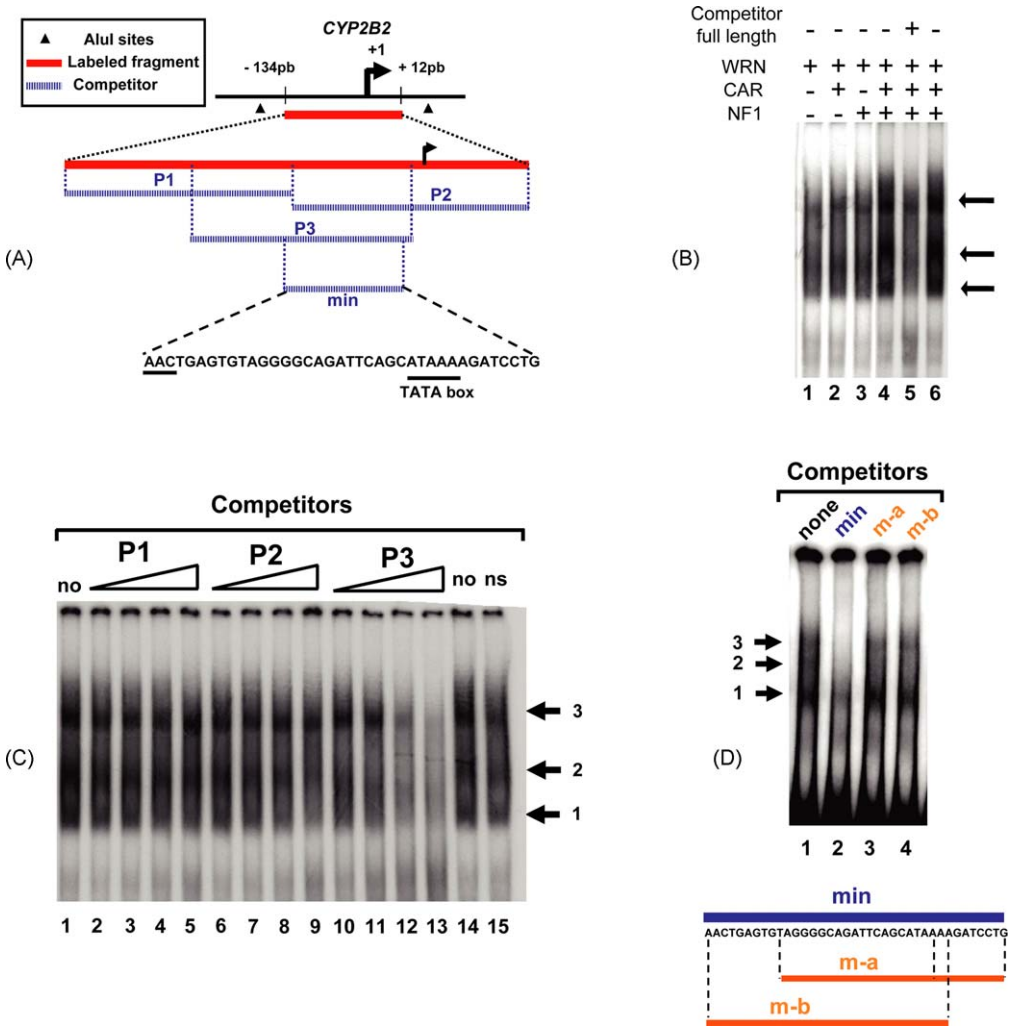

Fig. 4. WRN in combination with CAR and NF1 can form a complex in vitro on the *CYP2B2* promoter. (A) Schematic representation of the region surrounding the *CYP2B2* transcription start site showing the 146-bp fragment that was labeled for use in EMSA experiments. The localizations of unlabeled competitors P1, P2, P3 and min are also shown. The first three nucleotides of the min oligo (underlined) are missing from P2. (B) EMSA analysis in which the 146-bp fragment 1 was labeled and incubated in the presence of in vitro-synthesized WRN, CAR or NF1 as shown. The labeled and unlabeled 146-bp fragment was prepared by PCR amplification using the primers for fragment 1 (Supplementary Table 1). The labeled DNA fragment was amplified in the presence of ^{32}P-dCTP and purified using a Bio-Rad Biospin column (Bio-Rad, Mississauga, Canada). The full-length competitor was the unlabeled 146-bp fragment, added at 20-fold molar excess. Arrows identify specific retarded complexes. (C) Identification of a fragment containing a specific binding site for WRN-related complexes. The labeled 146-bp fragment was prepared by PCR amplification as in (A) and incubated in the presence of in vitro-synthesized WRN, CAR and NF1. The positions of synthetic oligo competitors P1, P2 and P3, purchased from Sigma–Aldrich (Oakville, Canada), are shown schematically in panel A and their sequences are shown in Supplementary Table 2. Competitors were added in 10- 25-, 50- and 100-fold excess. ns, non-specific competitor, a 187-bp fragment of mouse albumin cDNA amplified with primers shown in Supplementary Table 3. (D) Further localization of the binding site for WRN-related complexes. The labeled 146-bp fragment was prepared by PCR amplification as in (A) and incubated in the presence of in vitro-synthesized WRN, CAR and NF1. The position and sequence of the min competitor oligo (Sigma–Aldrich) is shown in panel A. Competitors were added in 100-fold excess.

was incubated together with CAR and NF1, three more distinct and more abundant retarded complexes (complexes 1–3) were evident (Fig. 4B, lanes 4 and 6). A 20-fold excess of the unlabeled 146-bp fragment diminished the intensity of the bands corresponding to the three retarded complexes (Fig. 4B, lane 5).

To localize the binding site of the WRN retarded complexes, sub-fragments P1, P2 and P3 of the 146-bp *CYP2B2* promoter fragment (Fig. 4A) were employed as competitors. P1 did not compete appreciably for the formation of the complexes (Fig. 4C, compare lanes 1 and 14 with lanes 2–5). P2 did not compete for the formation of complex 3, but exhibited modest competition for complexes 1 and 2 (Fig. 4C, compare lanes 1 and 14 with lanes 6–9). P3 was an effective competitor for all three complexes (Fig. 4C, compare lanes 1 and 14 with lanes 10–13). These experiments demonstrate the specificity of the formation of the WRN retarded complexes and localize the binding site(s) to the central portion of the 146-bp *CYP2B2* promoter fragment. The binding site was further localized using as competitors the min oligo (Fig. 4A and D), as well as two fragments thereof, m-a and m-b (Fig. 4D). The min oligo was an effective competitor (Fig. 4D, compare lane 2 with lane 1), whereas the m-a and m-b oligos were markedly less effective (Fig. 4D, compare lane 1 with lanes 3 and 4). Note that the efficacious competition by the min oligo (Fig. 4D) and the modest competition by P2 (Fig. 4C) indicate that the 5′ end of the binding site includes the 5′ extremity of the min fragment.

4. Discussion

The reduction observed here of CYP2B10 mRNA and protein in $Wrn^{\Delta hel/\Delta hel}$ mice is consistent with the reported reduction in transcriptional activity in human *WRN* mutant cells [13,14]. The recruitment of WRN to the *CYP2B2* promoter is consistent with the foregoing observations and suggests that WRN may play a positive role in *CYP2B* transcription. Note that the chromatin digestion

strategy employed here presents the double advantage of permitting greater reproducibility of chromatin shearing compared to classical sonication and more precise determination of the exact position(s) in the target DNA where the protein is bound [49]. Furthermore, with in situ perfusion, chromatin crosslinking occurs in vivo, assuring that WRN is in its native state at the moment when crosslinking occurs.

WRN is already known to interact with an impressive list of proteins, mostly involved in DNA repair, DNA replication and telomere maintenance [59]. To that list is now added a number of traditional transcription factors, particularly the nuclear receptors CAR, FXR and PXR, but also NF1, as they were co-immunoprecipitated with WRN by anti-WRN Ab. It is noteworthy that two of the transcription factors tested, C/EBPα and LXR, were not co-precipitated with WRN. Hence, despite the apparent promiscuity in WRN interactions with transcription factors observed here, there is selectivity. It is tempting to speculate that such selectivity is related to the reported selectivity of the genes affected in the WS transcription defect [14].

Perhaps the most surprising result, among several reported here, is the observation that retarded EMSA complexes are formed by WRN on the *CYP2B2* proximal promoter. At least three such complexes were observed here. It is possible that the multiple retarded complexes simply reflect the presence both in rat liver and in the in vitro-synthesized WRN product of a number of forms of lower molecular mass than the major form. Further experiments will be required to resolve this issue. The retarded complexes were better defined and more abundant in the presence of both CAR and NF1. There are no canonical binding sites for CAR or NF1 in the region of binding. Furthermore, although WRN is known to bind to a variety of non-canonical structures associated with DNA damage and DNA repair [60,61], it has little affinity for intact duplexes [61]. One possibility is that WRN, in association with proteins for which it has affinity as shown by the co-immunoprecipitation results, can acquire a sequence-specific DNA binding activity. But that interpretation is difficult to reconcile with the observation that it is not so much the position of the retarded complexes but their definition and amount that changes in the presence of CAR and NF1. One intriguing possibility is that CAR and NF1 stabilize WRN because they can bind to it (Fig. 3) in the reaction mixtures and thus increase the likelihood of complex formation between WRN and its target on the DNA. According to this interpretation it would be WRN itself that binds to DNA. It is not unreasonable to suggest that such binding could stimulate transcription of the adjacent gene(s), in this case rodent *CYP2B* genes. In any event, there is a WRN binding site in a region of DNA sequence to which WRN is recruited in vivo. This region contains the TATA box of the *CYP2B2* gene (Fig. 4A). Taken together, our results suggest that WRN participates in transcription of *CYP2B* genes in liver and identifies the first physical interaction between a specific promoter sequence and WRN.

Acknowledgments

The authors thank R.G. Evans, J.-A. Gustafsson and L. Bélanger for expression vectors, D. Waxman for the anti-CYP2B1 antibody, S. Roy for material, V. Stefanovsky for advice, and J. Côté for advice and encouragement. This work was supported by grants from the Instituts de recherche en santé du Canada to A. Anderson and to M. Lebel. M. Lebel is a senior scholar of the Fonds de recherche en santé du Québec.

Appendix A. Supplementary data

Supplementary data associated with this article can be found, in the online version, at doi:10.1016/j.bcp.2009.09.002.

References

[1] Martin GM. Genetic modulation of senescent phenotypes in *Homo sapiens*. Cell 2005;120:523–32.
[2] Epstein CJ, Motulsky AG. Werner syndrome: entering the helicase era. Bioessays 1996;18:1025–7.
[3] Goto M. Hierarchical deterioration of body systems in Werner's syndrome: implications for normal ageing. Mech Ageing Dev 1997;98:239–54.
[4] Yu CE, Oshima J, Fu YH, Wijsman EM, Hisama F, Alisch R, et al. Positional cloning of the Werner's syndrome gene. Science 1996;272:258–62.
[5] Gray MD, Shen JC, Kamath-Loeb AS, Blank A, Sopher BL, Martin GM, et al. The Werner syndrome protein is a DNA helicase. Nat Genet 1997;17:100–3.
[6] Imamura O, Ichikawa K, Yamabe Y, Goto M, Sugawara M, Furuichi Y. Cloning of a mouse homologue of the human Werner syndrome gene and assignment to 8A4 by fluorescence in situ hybridization. Genomics 1997;41:298–300.
[7] Kamath-Loeb AS, Shen JC, Loeb LA, Fry M. Werner syndrome protein. II. Characterization of the integral $3' \rightarrow 5'$ DNA exonuclease. J Biol Chem 1998;273:34145–50.
[8] Shen JC, Gray MD, Oshima J, Kamath-Loeb AS, Fry M, Loeb LA. Werner syndrome protein. I. DNA helicase and DNA exonuclease reside on the same polypeptide. J Biol Chem 1998;273:34139–44.
[9] Kudlow BA, Kennedy BK, Monnat Jr RJ. Werner and Hutchinson–Gilford progeria syndromes: mechanistic basis of human progeroid diseases. Nat Rev Mol Cell Biol 2007;8:394–404.
[10] Huang S, Lee L, Hanson NB, Lenaerts C, Hoehn H, Poot M, et al. The spectrum of WRN mutations in Werner syndrome patients. Hum Mutat 2006;27:558–67.
[11] Navarro CL, Cau P, Levy N. Molecular bases of progeroid syndromes. Hum Mol Genet 2006;15:R151–61.
[12] Bohr VA. Rising from the RecQ-age: the role of human RecQ helicases in genome maintenance. Trends Biochem Sci 2008;33:609–20.
[13] Balajee AS, Machwe A, May A, Gray MD, Oshima J, Martin GM, et al. The Werner syndrome protein is involved in RNA polymerase II transcription. Mol Biol Cell 1999;10:2655–68.
[14] Kyng KJ, May A, Kolvraa S, Bohr VA. Gene expression profiling in Werner syndrome closely resembles that of normal aging. Proc Natl Acad Sci USA 2003;100:12259–64.
[15] Turaga RV, Paquet ER, Sild M, Vignard J, Garand C, Johnson FB, et al. The Werner syndrome protein affects the expression of genes involved in adipogenesis and inflammation in addition to cell cycle and DNA damage responses. Cell Cycle 2009;8:2080–92.
[16] Kyng K, Croteau DL, Bohr VA. Werner syndrome resembles normal aging. Cell Cycle 2009;8:2323.
[17] Kwan P, Brodie MJ. Phenobarbital for the treatment of epilepsy in the 21st century: a critical review. Epilepsia 2004;45:1141–9.
[18] Okey AB. Enzyme induction in the cytochrome P-450 system. Pharmacol Ther 1990;45:241–98.
[19] Waxman DJ, Azaroff L. Phenobarbital induction of cytochrome P-450 gene expression. Biochem J 1992;281:577–92.
[20] Christou M, Wilson NM, Jefcoate CR. Expression and function of three cytochrome *P*-450 isozymes in rat extrahepatic tissues. Arch Biochem Biophys 1987;258:519–34.
[21] Wilson NM, Christou M, Jefcoate CR. Differential expression and function of three closely related phenobarbital-inducible cytochrome *P*-450 isozymes in untreated rat liver. Arch Biochem Biophys 1987;256:407–20.
[22] Anderson A. The induction of CYP2B proteins in rodents by phenobarbital-like inducers: what has been discovered and what remains to be learned. Acta Chim Slov 2008;55:45–52.
[23] Honkakoski P, Auriola S, Lang MA. Distinct induction profiles of 3 phenobarbital-responsive mouse liver cytochrome-P450 isozymes. Biochem Pharmacol 1992;43:2121–8.
[24] Hardwick JP, Gonzalez FJ, Kasper CB. Transcriptional regulation of rat liver epoxide hydratase, NADPH-cytochrome P-450 oxidoreductase, and cytochrome P-450b genes by phenobarbital. J Biol Chem 1983;258:8081–5.
[25] Rencurel F, Foretz M, Kaufmann MR, Stroka D, Looser R, Leclerc I, et al. Stimulation of AMP-activated protein kinase is essential for the induction of drug metabolizing enzymes by phenobarbital in human and mouse liver. Mol Pharmacol 2006;70:1925–34.
[26] Sueyoshi T, Negishi M. Phenobarbital response elements of cytochrome P450 genes and nuclear receptors. Annu Rev Pharmacol Toxicol 2001;41:123–43.
[27] Trottier E, Belzil A, Stoltz C, Anderson A. Localization of a phenobarbital responsive element (*PBRE*) in the 5′-flanking region of the rat *CYP2B2* gene. Gene 1995;158:263–8.
[28] Stoltz C, Vachon M-H, Trottier E, Dubois S, Paquet Y, Anderson A. The *CYP2B2* phenobarbital response unit contains an accessory factor element and a putative glucocorticoid response element essential for conferring maximal phenobarbital responsiveness. J Biol Chem 1998;273:8528–36.
[29] Hirsch-Ernst KI, Schlaefer K, Bauer D, Heder AF, Kahl GF. Repression of phenobarbital-dependent CYP2B1 mRNA induction by reactive oxygen species in primary rat hepatocyte cultures. Mol Pharmacol 2001;59:1402–9.
[30] Honkakoski P, Negishi M. Characterization of a phenobarbital-responsive enhancer module in mouse P450 *Cyp2b10* gene. J Biol Chem 1997;272:14943–9.
[31] Paquet Y, Trottier E, Beaudet M-J, Anderson A. Mutational analysis of the *CYP2B2* phenobarbital response unit and inhibitory effect of the constitutive

androstane receptor on phenobarbital responsiveness. J Biol Chem 2000;275: 38427–36.
[32] Honkakoski P, Moore R, Washburn KA, Negishi M. Activation by diverse xenochemicals of the 51-base pair phenobarbital-responsive enhancer module in the *CYP2B10* gene. Mol Pharmacol 1998;53:597–601.
[33] Beaudet M-J, Desrochers M, Lachaud AA, Anderson A. The *CYP2B2* phenobarbital response unit contains binding sites for hepatocyte nuclear protein 4, PBX-PREP1, the thyroid receptor, and the liver X receptor. Biochem J 2005;388:407–18.
[34] Honkakoski P, Zelko I, Sueyoshi T, Negishi M. The nuclear orphan receptor CAR-retinoid X receptor heterodimer activates the phenobarbital-responsive enhancer module of the *CYP2B* gene. Mol Cell Biol 1998;18:5652–8.
[35] Tzameli I, Pissios P, Schuetz EG, Moore DD. The xenobiotic compound 1,4-bis[2-(3,5-dichloropyridyloxy)]benzene is an agonist ligand for the nuclear receptor CAR. Mol Cell Biol 2000;20:2951–8.
[36] Zhang Q, Bae Y, Kemper JK, Kemper B. Analysis of multiple nuclear receptor binding sites for CAR/RXR in the phenobarbital responsive unit of CYP2B2. Arch Biochem Biophys 2006;451:119–27.
[37] Kawamoto T, Sueyoshi T, Zelko I, Moore R, Washburn K, Negishi M. Phenobarbital-responsive nuclear translocation of the receptor CAR in induction of the *CYP2B* gene. Mol Cell Biol 1999;19:6318–22.
[38] Wei P, Zhang J, Egan-Hafley M, Liang S, Moore DD. The nuclear receptor CAR mediates specific xenobiotic induction of drug metabolism. Nature 2000;407: 920–3.
[39] Lebel M, Leder P. A deletion within the murine Werner syndrome helicase induces sensitivity to inhibitors of topoisomerase and loss of cellular proliferative capacity. Proc Natl Acad Sci USA 1998;95:13097–102.
[40] Jean A, Rivkin E, Anderson A. Simple sequence DNA associated with near sequence identity of the 3′-flanking regions of rat cytochrome P450b and P450e genes. DNA 1988;7:361–9.
[41] Wrighton SA, Schuetz EG, Watkins PB, Maurel P, Barwick J, Bailey BS, et al. Demonstration in multiple species of inducible hepatic cytochromes P-450 and their mRNAs related to the glucocorticoid-inducible cytochrome P-450 of the rat. Mol Pharmacol 1985;28:312–21.
[42] Cherrington NJ, Slitt AL, Maher JM, Zhang XX, Zhang J, Huang W, et al. Induction of multidrug resistance protein 3 (MRP3) in vivo is independent of constitutive androstane receptor. Drug Metab Dispos 2004;31: 1315–9.
[43] Desrochers M, Christou M, Jefcoate C, Belzil A, Anderson A. New proteins in the rat CYP2B subfamily: presence in liver microsomes of the constitutive CYP2B3 protein and the phenobarbital-inducible protein product of alternatively spliced CYP2B2 mRNA. Biochem Pharmacol 1996;52:1311–9.
[44] Waxman DJ. Rat hepatic cytochrome P-450 isoenzyme 2c. Identification as a male-specific, developmentally induced steroid 16-hydroxylase and comparison to a female-specific cytochrome P-450 isoenzyme. J Biol Chem 1984;259: 15481–90.
[45] Wiwi CA, Gupte M, Waxman DJ. Sexually dimorphic P450 gene expression in liver-specific hepatocyte nuclear factor 4-deficient mice. Mol Endocrinol 2004;18:1975–87.
[46] Leenders F, Adamski J, Husen B, Thole HH, Jungblut PW. Molecular cloning and amino acid sequence of the porcine 17-estradiol dehydrogenase. Eur J Biochem 1994;222:221–7.
[47] Renwick AG, Soon CY, Chambers SM, Brown CR. Estradiol-17 dehydrogenase from chicken liver. J Biol Chem 1981;256:1881–7.
[48] Henderson LL, Warren JC. Purification and characterization of epimeric estradiol dehydrogenases (17 and 17) from equine placenta. Biochemistry 1984;23: 486–91.
[49] Chaya D, Zaret KS. Sequential chromatin immunoprecipitation from animal tissues. Methods Enzymol 2004;376:361–72.
[50] Seglen PO. Preparation of rat liver cells. 3. Enzymatic requirements for tissue dispersion. Exp Cell Res 1973;82:391–8.
[51] Massip L, Garand C, Turaga RV, Deschenes F, Thorin E, Lebel M. Increased insulin, triglycerides, reactive oxygen species, and cardiac fibrosis in mice with a mutation in the helicase domain of the Werner syndrome gene homologue. Exp Gerontol 2006;41:157–68.
[52] Anakk S, Kalsotra A, Kikuta Y, Huang W, Zhang J, Staudinger JL, et al. CAR/PXR provide directives for Cyp3a41 gene regulation differently from Cyp3a11. Pharmacogenom J 2004;4:91–101.
[53] Hartley DP, Klaassen CD. Detection of chemical-induced differential expression of rat hepatic cytochrome P450 mRNA transcripts using branched DNA signal amplification technology. Drug Metab Dispos 2005;28:608–16.
[54] Cheng WH, von Kobbe C, Opresko PL, Fields KM, Ren J, Kufe D, et al. Werner syndrome protein phosphorylation by Abl tyrosine kinase regulates its activity and distribution. Mol Cell Biol 2003;23:6385–95.
[55] Opresko PL, Cheng WH, von Kobbe C, Harrigan JA, Bohr VA. Werner syndrome and the function of the Werner protein; what they can teach us about the molecular aging process. Carcinogenesis 2003;24:791–802.
[56] Blander G, Kipnis J, Leal JF, Yu CE, Schellenberg GD, Oren M. Physical and functional interaction between p53 and the Werner's syndrome protein. J Biol Chem 1999;274:29463–9.
[57] Park Y, Kemper B. The *CYP2B1* proximal promoter contains a functional C/EBP regulatory element. DNA Cell Biol 1996;15:693–701.
[58] Luc P-VT, Adesnik M, Ganguly S, Shaw PM. Transcriptional regulation of the *CYP2B1* and *CYP2B2* genes by C/EBP-related proteins. Biochem Pharmacol 1996;51:345–56.
[59] Kusumoto R, Muftuoglu M, Bohr VA. The role of WRN in DNA repair is affected by post-translational modifications. Mech Ageing Dev 2007;128:50–7.
[60] von Kobbe C, Thoma NH, Czyzewski BK, Pavletich NP, Bohr VA. Werner syndrome protein contains three structure-specific DNA binding domains. J Biol Chem 2003;278:52997–3006.
[61] Shen JC, Loeb LA. Werner syndrome exonuclease catalyzes structure-dependent degradation of DNA. Nucleic Acids Res 2000;28:3260–8.